Evidence That a Minor Groove-Binding Peptide and a Major Groove-Binding Protein Can Simultaneously Occupy a Common Site on DNA†

Martha G. Oakley, Milan Mrksich, and Peter B. Dervan*

Arnold and Mabel Beckman Laboratories of Chemical Synthesis, Division of Chemistry and Chemical Engineering, California Institute of Technology, Pasadena, California 91125

Received May 18, 1992; Revised Manuscript Received August 24, 1992

ABSTRACT: Affinity cleaving proteins have been synthesized based on the DNA-binding domain of the yeast transcriptional activator GCN4 with the DNA cleaving moiety Fe·EDTA attached at the NH_2 terminus [Oakley, M. G., & Dervan, P. B. (1990) *Science 248*, 847]. Cleavage patterns generated by Fe·EDTA–GCN4(226–281) bound to the DNA sites 5′-CTGACTAAT-3′ and 5′-ATGACTCTT-3′ reveal that the NH_2 termini of the GCN4 DNA-binding domain are located in the major groove of DNA, 9–10 base pairs apart, consistent with a Y-shaped dimeric structure. 1-Methylimidazole-2-carboxamide netropsin (2-ImN) is a designed synthetic peptide which binds in the minor groove of DNA at 5′-TGACT-3′ sites as an antiparallel, side-by-side dimer [Mrksich, M., Wade, W. S., Dwyer, T. J., Geierstanger, B. H., Wemmer, D. E., & Dervan, P. B. (1992) *Proc. Natl. Acad. Sci. U.S.A. 89*, 7586]. Through the use of Fe·EDTA–GCN4(226–281) as a sequence-specific footprinting agent, it is shown that the dimeric protein GCN4-(226–281) and the dimeric peptide 2-ImN can simultaneously occupy their common binding site in the major and minor grooves of DNA, respectively. The association constants for 2-ImN in the presence and in the absence of Fe·EDTA–GCN4(226–281) are found to be similar, suggesting that the binding of the two dimers is not cooperative.

GCN4 is a yeast transcriptional activator responsible for the coordinate induction of 30–50 genes involved in amino acid biosynthesis in response to amino acid starvation (Jones & Fink, 1982). This protein is a member of a class of sequence-specific DNA-binding proteins known as the leucine zipper–basic region proteins, which are proposed to bind to DNA through a conserved structural motif consisting of a coiled coil dimerization domain, often termed the leucine zipper, and a DNA-binding domain termed the basic region (Landschulz et al., 1988, 1989; Kouzarides & Ziff, 1988; Sassone-Corsi et al., 1988; Gentz et al., 1989; Neuberg et al., 1989; O'Shea et al., 1989, 1991; Turner & Tjian, 1989; Vinson et al., 1989; O'Neil et al., 1990; Talanian et al., 1990). These proteins recognize, as dimers, binding sites on DNA consisting of abutted inverted repeats. For GCN4, the consensus DNA-binding site is 5′-rrTGACTcatt-3′, where the underlined C corresponds to the center of pseudodyad symmetry (Hope & Struhl, 1985; Hill et al., 1986).

The C-terminal 60 amino acids of GCN4 (residues 222–281) contain both the leucine zipper and basic regions and have been shown to be necessary and sufficient for both dimerization and sequence-specific DNA binding (Hope & Struhl, 1986, 1987). Two detailed modeling studies of leucine zipper–basic region proteins have been reported: the scissors-grip model of Vinson et al. (1989) and the induced helical fork model of O'Neil et al. (1990). Although these structural models differ slightly, both propose exclusively major-groove binding. Footprinting, methylation interference, and ethylation interference studies are also consistent with largely major-groove binding by these proteins (Vinson et al., 1989; Gartenberg et al., 1990; Nye & Graves, 1990). Affinity cleaving proteins based on the DNA-binding domain of GCN4 with the DNA-cleaving moiety Fe·EDTA at the NH_2 terminus have been synthesized (Figure 1, A,B) (Oakley & Dervan, 1990). Cleavage patterns generated by Fe·EDTA–GCN4-(226–281) bound to the DNA sites 5′-CTGACTAAT-3′ and 5′-ATGACTCTT-3′ reveal that the NH_2 termini of the GCN4 DNA-binding domain are located in the major groove of DNA, 9–10 base pairs apart, consistent with a Y-shaped dimeric structure (Oakley & Dervan, 1990). However, the structure of the DNA-binding region of this class of proteins has not been determined by X-ray crystallography or by nuclear magnetic resonance spectroscopy.

1-Methylimidazole-2-carboxamide netropsin (2-ImN) is a synthetic analog of the naturally occurring minor-groove-binding peptide distamycin A, wherein the NH_2-terminal pyrrole has been replaced by 1-methylimidazole in order to allow for the binding of sites containing G,C base pairs (Figure 1C). Footprinting and affinity cleaving studies reveal that 2-ImN binds to the five base pair sequence 5′-TGACT-3′ (Wade et al., 1992), the conserved element of the GCN4 recognition site. Two-dimensional NMR studies have recently shown that 2-ImN binds to its recognition site in the minor groove of DNA as a side-by-side, antiparallel dimer (Mrksich et al., 1992), forming a complex similar to that observed for distamycin binding to a 5′-AAATT-3′ sequence at high concentrations (Pelton & Wemmer, 1989).

The complexes formed by 2-ImN and the GCN4 DNA-binding domain with their common DNA-binding site are shown schematically in Figure 2, panels A and B, respectively. The question arises as to whether these molecules can bind to their common DNA-binding site simultaneously (Figure 2C). This question of mutual recognition is addressed here by the use of Fe·EDTA–GCN4(226–281) as a sequence-specific footprinting reagent. Following chemical activation with a reducing agent such as dithiothreitol (DTT), Fe·EDTA localized in the major groove at a specific DNA-binding site

† This work was supported by the National Institutes of Health (GM-27681), the National Foundation for Cancer Research, a National Science Foundation predoctoral fellowship, and a National Institutes of Health predoctoral traineeship to M.G.O. and a National Institutes of Health Research Service Award to M.M.

0006-2960/92/0431-10969$03.00/0

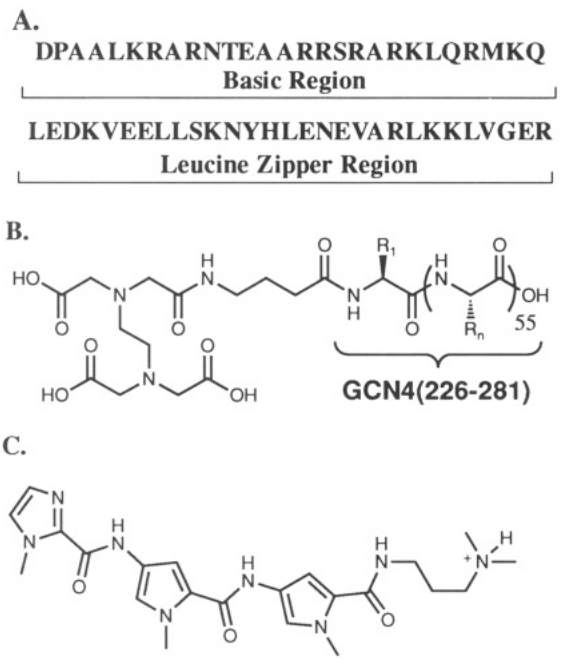

FIGURE 1: (A) Sequence of the carboxy-terminal 56 amino acids (226–281) of GCN4. The sequence is shown from the amino terminus of the peptide to its carboxy terminus. (B) Synthetic peptide EDTA–GCN4(226–281). (C) Synthetic minor-groove-binding peptide 2-ImN.

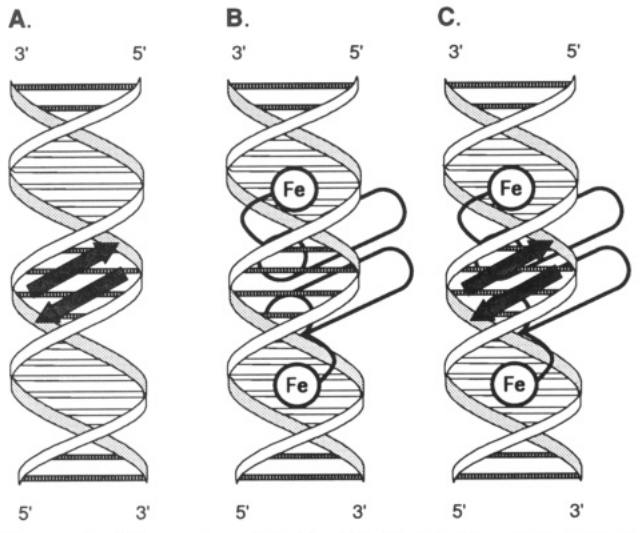

FIGURE 2: Schematic models for (A) the binding of the 2-ImN antiparallel dimer in the minor groove of DNA in which 2-ImN monomers are represented as arrows, (B) the leucine zipper DNA-binding motif in which the leucine zipper domains are represented by a pair of cylinders pointing into the DNA, and (C) both dimers binding to the same DNA molecule.

cleaves the proximal and distal strands of the adjacent minor grooves via a diffusible, non-sequence-specific radical, most likely hydroxyl (Taylor et al., 1984; Hertzberg & Dervan, 1984; Moser & Dervan, 1987; Oakley & Dervan, 1990). The cleavage pattern generated by the dimeric Fe·EDTA–GCN4-(226–281) extends beyond the five base pair recognition site for 2-ImN. Therefore, the peptide dimer bound in the minor groove should be capable of protecting its binding site from cleavage by diffusible radicals generated locally by Fe·EDTA–GCN4(226–281) bound at the same sequence in the major groove. This protection will be observed if, and only if, the major-groove-binding protein GCN4 and the minor-groove-binding synthetic peptide 2-ImN share their sites simultaneously on the same molecule of DNA.

MATERIALS AND METHODS

Materials

Protected amino acid derivatives were purchased from Peninsula Laboratories; Boc-L-His(DNP) was obtained from Fluka. Arg-(phenylacetamido)methyl (PAM) resin, *N*,*N*-dimethylformamide (DMF), diisopropylethylamine, dicyclohexylcarbodiimide in dichloromethane, *N*-hydroxybenzotriazole (HOBt) in DMF, and trifluoroacetic acid (TFA) were purchased from Applied Biosystems. Dichloromethane and methanol (HPLC grade) were obtained from Mallinckrodt, HOBt, *p*-cresol and *p*-thiocresol from Aldrich, and diethyl ether (low peroxide content) from Baker.

Doubly distilled water was further purified through the Milli Q filtration system from Millipore. Sonicated, deproteinized calf thymus DNA was purchased from Pharmacia and dissolved in H_2O to a concentration of 1 mM in base pairs. tRNA (*Escherichia coli* strain W, type XX) was obtained from Sigma and was dissolved in water and sterile-filtered. Enzymes were obtained from Boehringer-Mannheim or New England Biolabs and used with the buffers supplied. Glycogen was obtained from Boehringer-Mannheim. Deoxyadenosine 5′-[α-^{32}P]triphosphate and adenosine 5′-[γ-^{32}P]-triphosphate were obtained from Amersham. UV–vis spectra were recorded on a Hewlett-Packard Diode Array spectrophotometer. Cerenkov radioactivity was measured with a Beckman LS 3801 Scintillation Counter. Storage phosphor technology autoradiography was accomplished using a Molecular Dynamics 400S Phosphorimager and ImageQuant software. Storage phosphor screens (Kodak no. S0230) were purchased from Molecular Dynamics.

Methods

Peptide and Protein Syntheses. EDTA–GCN4(226–281) and GCN4(226–281) were synthesized, deprotected, and purified as previously described (Oakley & Dervan, 1990; Kent, 1988; Sluka et al., 1990a,b; Mack et al., 1990). NH_2-terminal sequencing of the purified GCN4(226–281) protein confirmed the desired sequence. Molecular masses (Da) were verified by electrospray mass spectrometry [GCN4(226–281): calculated mass, 6615.7; observed, 6615.1. EDTA–GCN4(226–281): calculated mass, 6975.0, Na complex, 6998.0, Fe complex, 7030.9; observed 6998.2, 7031.7]. 2-ImN was prepared and purified as previously described (Wade et al., 1992). Fe·EDTA–GCN4(226–281) was generated immediately prior to use by equilibration of 1 mM EDTA–GCN4(226–281) with an equal volume of 1 mM ferrous ammonium sulfate for approximately 10 min. Fe·EDTA–GCN4(226–281) was then diluted to a concentration of 25 μM.

DNA Manipulations. The 270 bp *Pvu*II–*Eco*RI restriction fragment of the plasmid pARE/GCRE (Harshman et al., 1988) was isolated and labeled at the 5′- or 3′-end by standard procedures (Sambrook et al., 1989). Chemical sequencing adenine-specific reactions were carried out as previously described (Iverson & Dervan, 1987). MPE·Fe reaction conditions were 20 mM phosphate, 20 mM NaCl, 5 mM DTT, 5 μM MPE·Fe, 100 μM calf thymus DNA, and 20 000 cpm labeled DNA, pH 7.5. The DNA-binding molecules were allowed to equilibrate with the DNA for 30 min. Reactions were then initiated by the addition of MPE·Fe, followed immediately by DTT, and allowed to proceed 10 min at room temperature. Affinity cleaving reaction conditions were 30 mM Tris·HCl, 3 mM sodium acetate, 20 mM NaCl, 5 mM DTT, 100 μM calf thymus DNA, and 20 000 cpm labeled

DNA, pH 7.9. 2-ImN was allowed to equilibrate with the DNA at room temperature for 30 min, at which point Fe·EDTA–GCN4(226–281) was added and allowed to equilibrate with the DNA for a further 30 min. The reactions were initiated with the addition of DTT and allowed to proceed at room temperature for 30 min. All reactions were terminated by ethanol precipitation; the residues were dried and resuspended in 100 mM tris-borate–EDTA/80% formamide loading buffer. Reaction products were analyzed by electrophoresis on 8% polyacrylamide denaturing gels (5% cross link, 7 M urea). After electrophoresis, gels were dried and autoradiographed. Gels were analyzed using storage phosphor technology. Storage phosphor screens were pressed against dried gels and exposed. A Molecular Dynamics 400S PhosphorImager was used to obtain data from storage screens, and data were analyzed by performing area integrations along lines drawn down the center of each lane using the ImageQuant v 3.0 software running on an AST Premium 386/33 computer.

Quantitative Footprint Titrations. The above reaction conditions were modified for quantitative footprinting as follows. tRNA was used in place of calf thymus DNA in order to minimize the binding of 2-ImN to carrier nucleic acid. Stock solutions of 2-ImN were diluted serially to give 15 solutions of concentrations ranging from 500 nM to 500 μM, leading to final reaction concentrations of 100 nM to 100 μM. Final reaction conditions were 30 mM Tris·HCl, 3 mM sodium acetate, 20 mM NaCl, 2 mM DTT, 100 μg/mL tRNA, 5 μM Fe·EDTA–GCN4(226–281) or 2.5 μM MPE-Fe, and 20 000 cpm 5′-^{32}P end-labeled DNA, pH 7.9. For MPE·Fe footprinting, 2-ImN was allowed to equilibrate at room temperature with the DNA for 1 h, followed by the addition of MPE·Fe and DTT. Reactions were quenched by ethanol precipitation after 30 min. For Fe·EDTA–GCN4(226–281) footprinting, 2-ImN was allowed to equilibrate with the DNA at room temperature for 45 min, followed by the addition of Fe·EDTA–GCN4(226–281). After 45 min, the reactions were initiated with DTT. Reactions were quenched by ethanol precipitation after a further 30 min.

Footprint Titration Fitting Procedure. The footprint titration gels were quantitated using storage phosphor technology, and data were analyzed by performing volume integrations of the target and reference sites using the ImageQuant v 3.0 software running on an AST Premium 386/33 computer. The target sites chosen were the two 5′-TGACT-3′ sites found in the restriction fragment. For the MPE·Fe footprint titrations, reference sites were chosen at which little 2-ImN binding was observed even at the highest concentrations, generally G,C-rich sites. For the Fe·EDTA–GCN4(226–281) footprint titration experiments, reference sites were taken from regions at each Fe·EDTA–GCN4(226–281) cleavage site at which the intensity of cleavage was unaltered. Specifically, the lower set of cleavage bands at each site was used: 5′-GGTT-3′ at the ARE site and approximately 5′-TAAAAA-3′ at the GCRE site.

The data from MPE·Fe and Fe·EDTA–GCN4(226–281) footprint titrations were analyzed using a method analogous to that described for analysis of DNase I footprint titrations (Brenowitz et al., 1986; Wade, 1989). The apparent DNA target site saturation, θ_{app}, was calculated using

$$\theta_{app} = 1 - \frac{I_{tot}/I_{ref}}{I_{tot}^{\circ}/I_{ref}^{\circ}} \quad (1)$$

where I_{tot} and I_{ref} are the integrated volumes of the target and reference sites, respectively, and I_{tot}° and I_{ref}° correspond to those values for an MPE·Fe or Fe·EDTA–GCN4(226–281) control lane to which no 2-ImN has been added. The ($[L]_{tot}$, θ_{app}) data points were fit by minimizing the difference between θ_{app} and θ_{fit}, using the modified Hill equation:

$$\theta_{fit} = \theta_{min} + (\theta_{max} - \theta_{min})\frac{K_a^2[L]_{tot}^2}{1 + K_a^2[L]_{tot}^2} \quad (2)$$

where $[L]_{tot}$ corresponds to the total 2-ImN concentration, K_a corresponds to the apparent monomeric association constant, and θ_{min} and θ_{max} represent the experimentally determined site saturation values when the site is unoccupied or saturated, respectively.

Data were fit using a nonlinear least-squares fitting procedure of KaleidaGraph software (version 2.1, Abelbeck

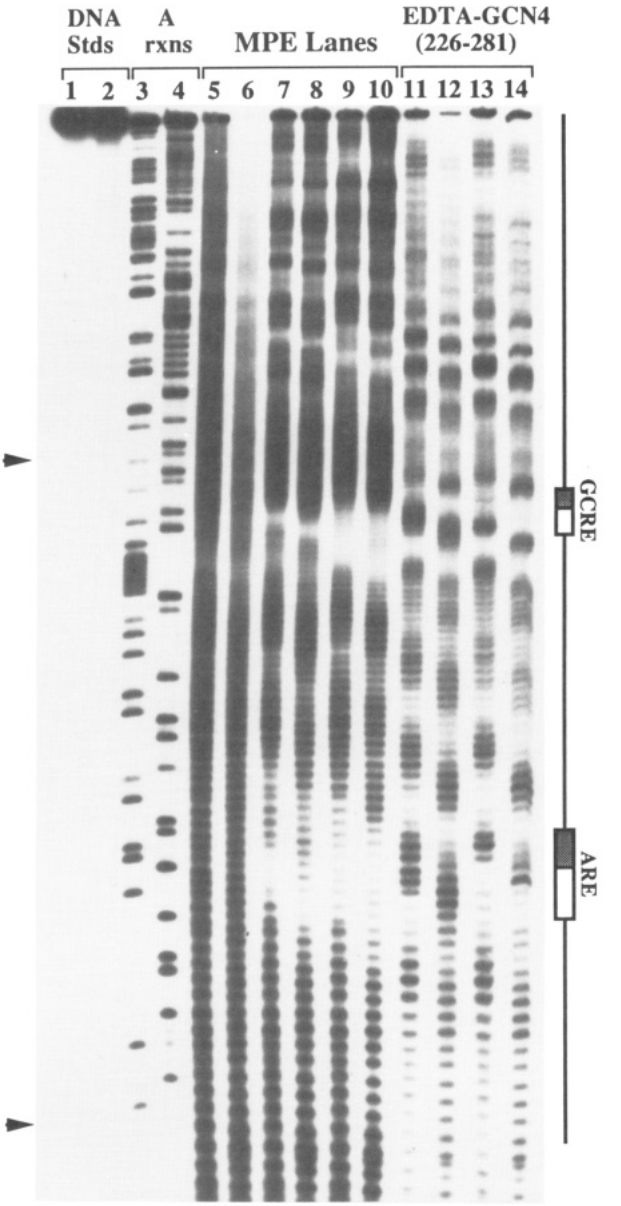

FIGURE 3: Autoradiogram of a high-resolution denaturing polyacrylamide gel of 2-ImN and GCN4(226–281) footprinting and of Fe·EDTA–GCN4(226–281) affinity cleaving reactions in the presence and absence of 2-ImN. Odd numbered lanes are 5′-end-labeled, and even numbered lanes are 3′-end-labeled. Lanes 1 and 2, DNA control lanes; lanes 3 and 4, A-specific chemical sequencing lanes; lanes 5 and 6, MPE·Fe control lanes; lanes 7 and 8, MPE·Fe cleavage protection by GCN4(226–281) (5 μM); lanes 9 and 10, MPE·Fe cleavage protection by 2-ImN (50 μM); lanes 11 and 12, Fe·EDTA–GCN4(226–281) at 5 μM; lanes 13 and 14, Fe·EDTA–GCN4(226–281) at 5 μM in the presence of 2-ImN at 50 μM.

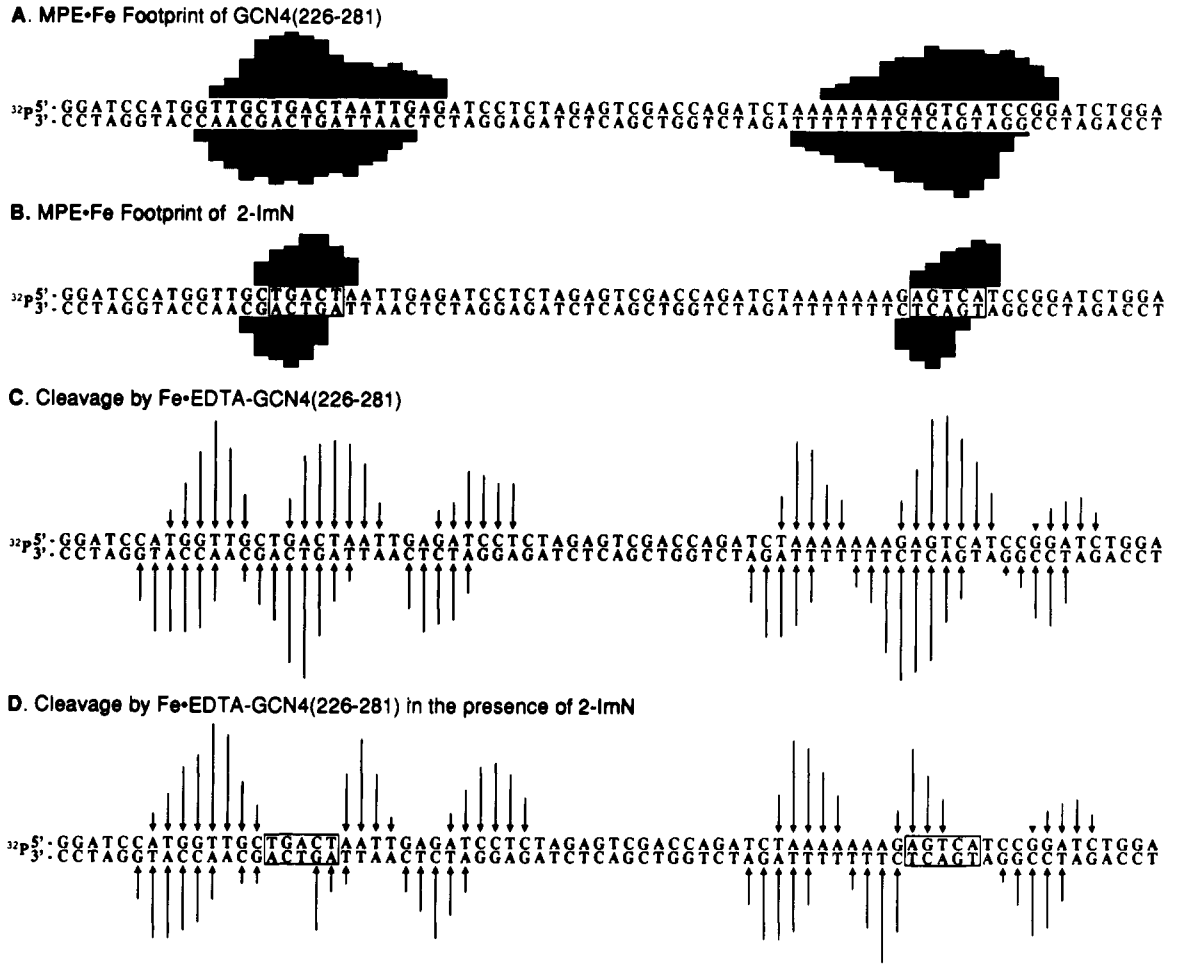

FIGURE 4: The sequence from left to right represents the data between the markers on the left-hand side of the gel shown in Figure 3. (A) Bars represent the extent of protection from MPE·Fe cleavage at the ARE and GCRE sites in the presence of 5 μM GCN4(226–281) (Figure 3, lanes 7 and 8). (B) Bars represent the extent of protection from MPE·Fe cleavage at the ARE and GCRE sites in the presence of 2-ImN (50 μM); boxes denote 2-ImN binding sites (Figure 3, lanes 9 and 10). (C) Arrows represent the extent of cleavage at the ARE and GCRE sites for Fe·EDTA–GCN4(226–281) at 5 μM (Figure 3, lanes 11 and 12). (D) Arrows represent the extent of cleavage at the ARE and GCRE sites for Fe·EDTA–GCN4(226–281) at 5 μM in the presence of 2-ImN (50 μM); boxes denote 2-ImN binding sites (Figure 3, lanes 13 and 14).

software) running on a Macintosh IIfx computer with K_a, θ_{max}, and θ_{min} as the adjustable parameters. All lanes from each gel were used unless visual inspection of the computer image from a storage phosphor screen revealed a flaw at the target or reference site or unless the θ_{app} value was greater than two standard errors away from values in both neighboring lanes and greater than two standard errors from the initial θ_{fit}. Data for experiments in which fewer than 80% of the lanes were usable were discarded. The data were normalized using

$$\theta_{norm} = \frac{\theta_{app} - \theta_{min}}{\theta_{max} - \theta_{min}} \quad (3)$$

The uncertainty in θ_{norm} was estimated from the scatter in the normalized data for the four lowest and four highest concentrations of 2-ImN. A standard uncertainty in θ_{norm} of 0.07 was used in a χ^2 analysis of normalized data, with $\chi^2 \leq 1.0$ as the criterion for an acceptable fit. Three or four sets of acceptable data were used in determining each association constant.

RESULTS AND DISCUSSION

Simultaneous Binding of 2-ImN and GCN4. Footprinting and affinity cleaving assays were performed on a restriction fragment (*Eco*RI–*Pvu*II) from the plasmid pARE/GCRE (Hashman et al., 1988) which was separately 5′- and 3′-^{32}P-end-labeled at the *Eco*RI site. This DNA fragment contains two binding sites for GCN4 and 2-ImN, 5′-CTGACTAAT-3′ and 5′-ATGACTCTT-3′, previously designated ARE and GCRE, respectively (Harshman et al., 1988). The DNA cleavage products were separated by polyacrylamide gel electrophoresis and visualized by autoradiography (Figure 3). From MPE·Fe footprinting, 2-ImN protects a region of approximately five base pairs at the site 5′-TGACT-3′ (Figure 3, lanes 7 and 8; Figure 4B), consistent with previous footprinting and affinity cleaving data (Wade et al., 1992) and direct NMR studies (Mrksich et al., 1992). GCN4-(226–281) protects an 18 bp region which contains the same five base-pair site, 5′-TGACT-3′. Importantly, the products of cleavage by Fe·EDTA–GCN4(226–281) in the absence and in the presence of 2-ImN differ (Figure 3, lanes 11–14; Figure 4C,D). The tripartite cleavage pattern for Fe·EDTA–GCN4(226–281) results from cleavage of the DNA-binding site by two Fe·EDTA moieties localized in successive major grooves (Figure 6A) (Oakley & Dervan, 1990). The cleavage pattern extends well beyond the five base-pair binding site for 2-ImN in both directions. Comparisons of lane 11 with lane 13 and lane 12 with lane 14 demonstrate that the intensity of cleavage is reduced dramatically in the central region of the cleavage pattern in the presence of 2-ImN. This cleavage pattern is unaltered upon changing the order of addition of

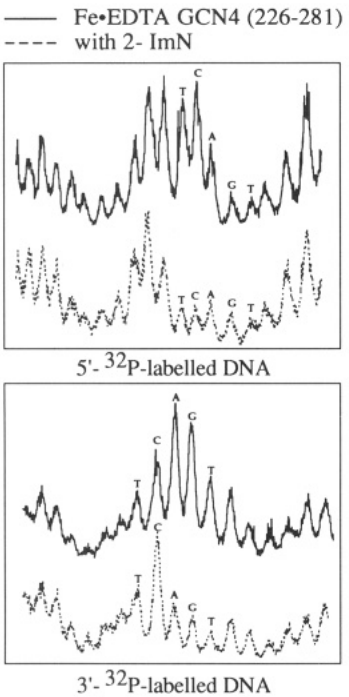

FIGURE 5: Phosphor storage densitometry traces of the 5′-TGACT-3′ sequence from the lower binding site (ARE) in lanes 11–14 of Figure 3. The solid lines show the data obtained from cleavage of the DNA with Fe•EDTA–GCN4(226–281) in the absence of 2-ImN; the dashed lines show the data obtained in the presence of 2-ImN. The peaks corresponding to the sequence 5′-TGACT-3′ are indicated.

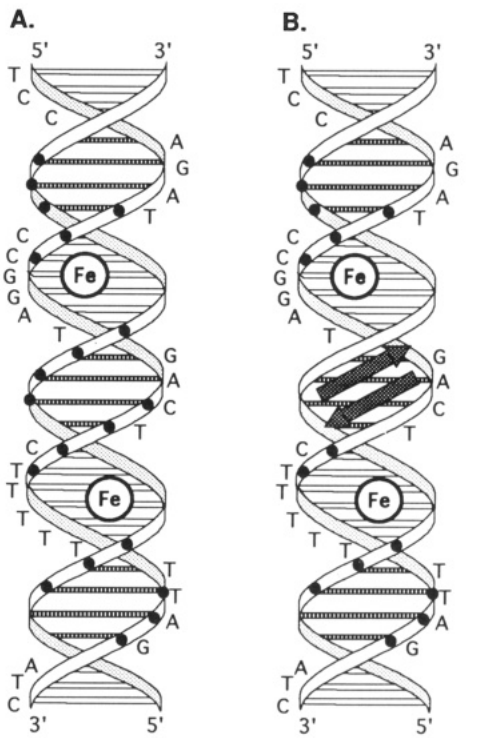

FIGURE 6: (A) Schematic for B-form DNA indicating the most intense cleavage sites for Fe•EDTA–GCN4(226–281) at the GCRE site. Filled circles represent the points of cleavage along the phosphodiester backbone. (B) Map of the most intense cleavage sites for Fe•EDTA–GCN4(226–281) in the presence of 2-ImN.

the two DNA-binding molecules (data not shown). The histograms in Figure 4 panels C and D and the densitometry traces in Figure 5 compare the cleavage patterns observed in the presence and absence of 2-ImN. The base positions at which cleavage intensity is reduced correspond to those bases protected by 2-ImN from cleavage by MPE•Fe, demonstrating that 2-ImN is capable of binding in the presence of Fe•EDTA–GCN4(226–281).

It is important to note that the altered cleavage pattern observed in Figure 4D can only occur if the two molecules occupy their common bindng site *simultaneously*. If binding by 2-ImN in the minor groove prevents Fe•EDTA–GCN4-(226–281) from binding in the major groove, no specific cleavage will be observed. Similarly, if binding by Fe•EDTA–GCN4(226–281) in the major groove prevents 2-ImN from binding in the minor groove, an unaltered cleavage pattern will be observed (Figure 3D). Furthermore, the cleavage intensity in the upper and lower sections of the tripartite Fe•EDTA–GCN4(226–281) cleavage pattern, which do not overlap a TGACT sequence, serves as an internal control for a decrease in the binding affinity of Fe•EDTA–GCN4(226–281) in the presence of 2-ImN. As can be seen from the data (Figure 3; Figure 4C,D), these bands are of similar intensity in the presence and absence of 2-ImN. The cleavage pattern for Fe•EDTA–GCN4(226–281) in the presence and absence of 2-ImN is shown mapped to a DNA double helix in Figure 6.

DNA Structure. This example of simultaneous sequence-specific complexation of a shared DNA-binding site by a protein and a small molecule is in contrast to results seen with related systems. The minor-groove binder distamycin inhibits cleavage by restriction endonucleases (Nosikov et al., 1976) and topoisomerase II (Fesen & Pommier, 1989) at A,T-rich sites. In addition, distamycin has been shown to inhibit the binding of regulatory proteins such as OTF-1, NFE-1 (Broggini et al., 1989), and the homeodomain proteins Ftz and Antp (Dorn et al., 1992). Surprisingly, distamycin is able to disrupt binding of a Ftz homeodomain peptide lacking the NH_2-terminal arm involved in minor-groove-specific contacts, implying that direct competition for the minor-groove-binding site is not required for inhibition (Dorn et al., 1992). It is proposed that the protein binding affinity is also reduced by a distamycin-induced conformational change in the local DNA structure (Dorn et al., 1992).

It is of interest to understand how the DNA is able to accommodate structurally the two dimeric species, GCN4 and 2-ImN. The simplest assumption is that different faces of the same local DNA structure are recognized by both dimers. Although some members of the leucine zipper–basic region class of DNA-binding proteins have been shown to bend their DNA recognition sites either toward (jun–jun homodimers) or away from (jun–fos heterodimers) the minor groove (Kerppola & Curran, 1991a,b), similar studies with GCN4 gave no evidence of protein-induced DNA bending (Gartenberg et al., 1990). Similarly, NMR studies with 2-ImN are consistent with no major distortion of the DNA double helix as a result of ligand binding (Mrksich et al., 1992).

Nevertheless, modeling studies indicate that the minor-groove width in the 2-ImN•5′-TGACT-3′ complex may be larger than that observed for canonical B-form DNA in order to accommodate the 2-ImN dimer (Mrksich et al., 1992). If even modest structural changes are induced upon binding of either the GCN4 or the 2-ImN dimer, positive or negative cooperativity between GCN4 and 2-ImN might be expected. In order to address this possibility, we have measured the binding affinity constants for 2-ImN in the presence and in the absence of Fe•EDTA–GCN4(226–281). To measure the apparent association constant of 2-ImN for each site in the absence of Fe•EDTA–GCN4(226–281), we used a quantitative MPE•Fe footprint titration procedure (Wade, 1989), adapted from the quantitative DNase footprint titration procedure of

Table I: Binding Constants for 2-ImN at Two DNA-Binding Sites Measured by Footprint Titrations Using Fe·EDTA–GCN4(226–281) and MPE·Fe

site	footprinting agent	K_{app} (M^{-1})[a,b]
5′-CTGACTCTT-3′	Fe·EDTA–GCN4(226–281)	2.2 (0.3) × 10^5
	MPE	1.5 (0.4) × 10^5
5′-ATGACTAAT-3′	Fe·EDTA–GCN4(226–281)	2.3 (0.6) × 10^5
	MPE	2.2 (0.5) × 10^5

[a] Values reported are the mean values measured from three or four footprint titration experiments. Numbers in parentheses indicate the standard deviation for the data set. [b] The assays were performed at room temperature, pH 7.9, in the presence of 30 mM Tris·HCl, 3 mM sodium acetate, and 20 mM sodium chloride.

Ackers and co-workers (Brenowitz et al., 1986). To measure the apparent association constant for each binding site in the presence of Fe·EDTA–GCN4(226–281), we used the protein itself as a site-specific footprinting agent.

Because NMR (Mrksich et al., 1992) and affinity cleaving (Wade et al., 1992) experiments support the assumption of all-or-none binding, apparent fractional saturation values (θ_{app}, eq 1) were fit to a modified Hill equation (eq 2)[1] (Cantor & Schimmel, 1980). The means of the best-fit apparent monomeric association constants are listed in Table I; the corresponding binding isotherms are shown in Figure 7. The association constants for 2-ImN in the presence and absence of Fe·EDTA–GCN4(226–281) differ by less than a factor of 2 at both sites and probably are not different within the error of the experiment. These data indicate that there is little, if any, cooperativity between the two molecules, supporting a model in which neither the 2-ImN dimer nor the truncated GCN4 dimer perturbs the common DNA-binding site significantly.

CONCLUSION

The DNA-binding domain of the leucine zipper–basic region protein GCN4 and the synthetic minor groove-binding peptide 2-ImN can bind to their common DNA-binding site simultaneously. This result supports models in which leucine zipper–basic region proteins bind to their DNA-binding sites exclusively in the major groove, leaving the minor groove unoccupied. Furthermore, binding of Fe·EDTA–GCN4(226–281) in the major groove has little or no effect on the equilibrium binding constant for 2-ImN. This demonstration that both grooves of the DNA may be occupied without significantly weakening the binding affinity of the major- or minor-groove-binding molecules suggests that tight-binding synthetic molecules may be designed with components interacting with both grooves of DNA over a limited sequence space.

ACKNOWLEDGMENT

We thank C. S. Parker for the gift of the plasmid pARE/GCRE, S. R. Wilson (New York University) for electrospray mass spectral analysis, and S. F. Singleton and W. S. Wade for helpful discussions.

[1] Data were also fit to

$$\theta_{fit} = \theta_{min} + (\theta_{max} - \theta_{min})\frac{K_1[L]_{tot} + K_1K_2[L]_{tot}^2}{1 + K_1[L]_{tot} + K_1K_2[L]_{tot}^2} \quad (4)$$

where K_1 corresponds to the association constant for binding of the first 2-ImN monomer and K_2 to the association constant for binding of the second monomer to a singly occupied site. Nonlinear least-squares analysis using eq 4 with K_1, K_2, θ_{min}, and θ_{max} as adjustable parameters resulted in fits of similar quality to those obtained using eq 2. Moreover, these results gave $K_2 \geq 1000K_1$, and $K_1K_2 \cong K_a^2$, justifying our use of an all-or-none approximation.

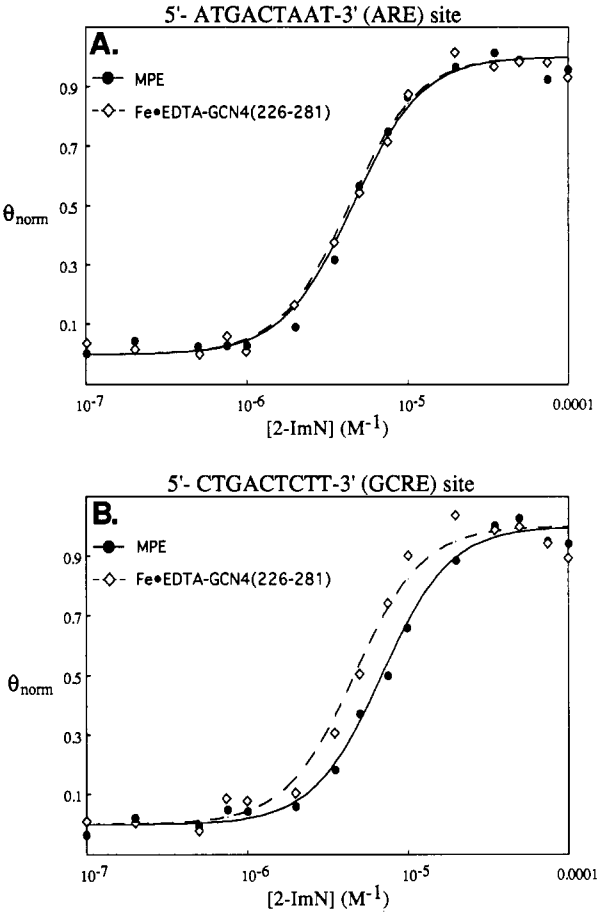

FIGURE 7: Data for the MPE·Fe and Fe·EDTA–GCN4(226–281) quantitative footprinting experiments at (A) the ARE site and (B) the GCRE site. The sigmoidal curves show the titration binding isotherms plotted with eq 2 using $\theta_{min} = 0$, $\theta_{max} = 1$, and the mean K_a value for each set (Table I). The solid curves represent the MPE·Fe footprinting data, the dotted curves the Fe·EDTA–GCN4(226–281) data. The data points are taken from the average of the normalized θ_{app} values at each concentration of 2-ImN; filled circles correspond to MPE·Fe data, open diamonds to Fe·EDTA–GCN4(226–281) data.

REFERENCES

Brenowitz, M., Senear, D. F., Shea, M. A., & Ackers, G. K. (1986) *Methods Enzymol. 130*, 132.

Broggini, M., Ponti, M., Ottolenghi, S., D'Incalci, M., Mongelli, N., & Mantovani, R. (1989) *Nucleic Acids Res. 17*, 1051.

Cantor, C. R., & Schimmel, P. R. (1980) *Biophysical Chemistry*, pp 863–866, W. H. Freedman and Company, New York.

Dorn, A., Affolter, M., Müller, M., Gehring, W. J., & Leupin, W. (1992) *EMBO J. 11*, 279.

Fesen, M., & Pommier, Y. (1989) *J. Biol. Chem. 264*, 11354.

Gartenberg, M. R., Ampe, C., Steitz, T. A., & Crothers, D. M. (1990) *Proc. Natl. Acad. Sci. U.S.A. 87*, 6034.

Gentz, R., Rauscher, F. J., Abate, C., & Curran, T. (1989) *Science 243*, 1695.

Harshman, K. D., Moye-Rowley, W. S., & Parker, C. S. (1988) *Cell 53*, 321.

Hertzberg, R. P., & Dervan, P. B. (1984) *Biochemistry 23*, 3934.

Hill, D. E., Hope, I. A., Macke, J. P., & Struhl, K. (1986) *Science 224*, 451.

Hope, I. A., & Struhl, K. (1985) *Cell 43*, 177.

Hope, I. A., & Struhl, K. (1986) *Cell 46*, 885.

Hope, I. A., & Struhl, K. (1987) *EMBO J. 6*, 2781.

Iverson, B., & Dervan, P. (1987) *Nucleic Acids Res. 15*, 7823.

Jones, E. W., & Fink, G. R. (1982) in *The Molecular Biology of the Yeast Saccharomyces: Metabolism and Gene Expression* (Strathern, J. N., Jones, E. W., & Broach, J. R., Eds.) p 181, Cold Spring Harbor Press, Col Spring Harbor, NY.
Kent, S. B. H. (1988) *Annu. Rev. Biochem. 57*, 957.
Kerppola, T. K., & Curran, T. (1991a) *Cell 66*, 317.
Kerppola, T. K., & Curran, T. (1991b) *Science 254*, 1210.
Kouzarides, T., & Ziff, E. (1988) *Nature 336*, 646.
Landschulz, W. H., Johnson, P. F., & McKnight, S. L. (1988) *Science 240*, 1759.
Landschulz, W. H., Johnson, P. F., & McKnight, S. L. (1989) *Science 243*, 1681.
Mack, D. P., Sluka, J. P., Shin, J. A., Griffin, J. H., Simon, M. I., & Dervan, P. B. (1990) *Biochemistry 29*, 6561.
Moser, H. E., & Dervan, P. B. (1987) *Science 238*, 645.
Mrksich, M., Wade, W. S., Dwyer, T. J., Geierstanger, B. H., Wemmer, D. E., & Dervan, P. B. (1992) *Proc. Natl. Acad. Sci. U.S.A. 89*, 7586.
Neuberg, M., Schuermann, M., Hunter, J. B., & Müller, R. (1989) *Nature 338*, 589.
Nosikov, V. V., Braga, E. A., Karlishev, A. V., Zhuze, A. L., & Polyanovsky, O. L. (1976) *Nucleic Acids Res. 3*, 2293.
Nye, J. A., & Graves, B. J. (1990) *Proc. Natl. Acad. Sci. U.S.A. 87*, 3992.
Oakley, M. G., & Dervan, P. B. (1990) *Science 248*, 847.
O'Neil, K. T., Hoess, R. H., & DeGrado, W. F. (1990) *Science 249*, 774.
O'Shea, E. K., Rutkowski, R., & Kim, P. S. (1989) *Science 243*, 538.
O'Shea, E. K., Klemm, J. D., Kim, P. S., & Alber, T. (1991) *Science 254*, 539.
Pelton, J. G., & Wemmer, D. E. (1989) *Proc. Natl. Acad. Sci. U.S.A. 86*, 5723.
Sambrook, J., Fritsch, E. F., & Maniatis, T. (1989) *Molecular Cloning: A Laboratory Manual*, 2nd ed., Cold Spring Harbor Press, Cold Spring Harbor, NY.
Sarin, V. K., Kent, S. B. H., Tam, J. P., & Merrifield, R. B. (1981) *Anal. Biochem. 117*, 147.
Sassone-Corsi, P., Ransone, L. J., Lamph, W. W., & Verma, I. (1988) *Nature 336*, 692.
Sluka, J. P., Griffin, J. H., Mack, D. P., & Dervan, P. B. (1990a) *J. Am. Chem. Soc. 112*, 6369.
Sluka, J. P., Horvath, S. J., Glasgow, A. C., Simon, M. I., & Dervan, P. B. (1990b) *Biochemistry 29*, 6561.
Talanian, R. V., McKnight, C. J., & Kim, P. S. (1990) *Science 249*, 769.
Taylor, J., Schultz, P., & Dervan, P. (1984) *Tetrahedron 40*, 457.
Turner, R., & Tjian, R. (1989) *Science 243*, 1689.
Umemoto, K., Sarma, M. H., Gupta, G., Luo, J., & Sarma, R. H. (1990) *J. Am. Chem. Soc. 112*, 4539.
Vinson, C. R., Sigler, P. B., & McKnight, S. L. (1989) *Science 246*, 911.
Wade, W. S. (1989) Ph.D. Thesis, California Institute of Technology, Pasadena, CA.
Wade, W. S., Mrksich, M., & Dervan, P. B. (1992) *J. Am. Chem. Soc.* (in press).